

## Fission Product Yield in the Neutron-Induced Fission of $^{232}\text{Th}$ with Average Energies of 5.42, 7.75, and 10.09 MeV

P. M. Prajapati\*

*M. S. University of Baroda, Faculty of Science, Physics Department  
Vadodara – 390 002, India*

H. Naik

*Bhabha Atomic Research Centre, Radiochemistry Division  
Mumbai – 400 085, India*

S. Mukherjee

*M. S. University of Baroda, Faculty of Science, Physics Department  
Vadodara – 390 002, India*

S. V. Suryanarayana

*Bhabha Atomic Research Centre, Nuclear Physics Division  
Mumbai – 400 085, India*

B. S. Shivashankar

*Manipal University, Department of Statistics  
Manipal – 576 104, India*

R. Crasta

*Mangalore University, Microtron Centre, Department of Studies in Physics  
Mangalagangothri – 574 199, India*

V. K. Mulik

*University of Pune, Department of Physics  
Pune – 411 007, India*

K. C. Jagadeesan and S. V. Thakre

*Bhabha Atomic Research Centre, Radiopharmaceutical Division  
Mumbai – 400 085, India*

---

\*E-mail: paresh\_21soft@yahoo.co.in

S. Ganesan

Bhabha Atomic Research Centre, Reactor Physics Design Division  
Mumbai – 400 085, India

and

A. Goswami

Bhabha Atomic Research Centre, Radiochemistry Division  
Mumbai – 400 085, India

Received August 11, 2012

Accepted April 11, 2013

doi:10.13182/NSE12-78

**Abstract**—The yields of various fission products in the neutron-induced fission of  $^{232}\text{Th}$  have been determined using a recoil catcher and off-line gamma-ray spectrometric technique with flux-averaged energies of 5.42, 7.75, and 10.09 MeV. The neutrons were generated using the  $^7\text{Li}(p,n)$  reaction at the BARC-TIFR [Bhabha Atomic Research Centre–Tata Institute of Fundamental Research] Pelletron facility, Mumbai, India. The fission product–yield data in the 10.09-MeV neutron-induced fission of  $^{232}\text{Th}$  are determined for the first time. The yields of the different fission products in the neutron-induced fission of  $^{232}\text{Th}$  with flux-averaged energies of 5.42 and 7.75 MeV from the present work have been compared with similar data of comparable neutron energy from the literature and are found to be in good agreement. The effect of nuclear structure on fission product yields as a function of neutron energy has been examined.

## I. INTRODUCTION

A major problem in the further development of nuclear power is governmental concerns arising from nuclear waste disposal schemes involving long-term geological storage of commercial reactor waste. Consequently, for future growth of nuclear power, it will be necessary to satisfactorily address the troublesome issue of disposal of nuclear waste. A fuel cycle based on thorium can address both these issues owing to a number of favorable neutronics and material characteristics that make thorium a better fertile host.<sup>1</sup> The  $^{232}\text{Th}$ – $^{233}\text{U}$  fuel cycle is advantageous to current reactors that are based on uranium fuel because the waste production of the  $^{232}\text{Th}$ – $^{233}\text{U}$  fuel cycle is a thousand times less radiotoxic. Further, thorium in its natural form consists of almost all  $^{232}\text{Th}$  with some trace amounts of  $^{230}\text{Th}$ . The occurrence of  $^{232}\text{Th}$  in the earth's crust is nearly three times that of uranium. Thus, thorium is an attractive fuel option regarding large-scale global deployment of nuclear energy to meet rising demands. An accelerator-driven subcritical system<sup>2–4</sup> (ADSS) based on the Th-U fuel cycle is relevant because one can exploit its potential for a hybrid reactor system that can produce nuclear power using thorium as a main fuel.

The development of ADSS and an advanced reactor program requires a significant amount of new and improved nuclear data<sup>5</sup> in extended energy regions as well as for a variety of new materials. Accurate nuclear

data such as fission yields, neutron capture cross sections, fission cross sections, and decay data including half-lives, decay energies, and branching ratio are required for many advanced reactor calculations. Further, the advent and development of advanced reactors have highlighted the need for accurate determination of fission yields in the fission of actinides induced by neutrons.

In any nuclear reactor, the neutron spectrum has the continuous energy ranging from 0 to 15 MeV, which depends upon the particular reactor design, whereas in ADSS the neutron energy goes up to 200 MeV and higher. This is because in ADSS, high-energy (giga-electron-volt) protons from an accelerator strike a heavy-element target like Pb or Bi, which yields a large number of high-energy neutrons by spallation reaction. Thus,  $^{232}\text{Th}$ – $^{233}\text{U}$  fuel in connection with ADSS has to face a wide range of neutron energies. The high-energy neutrons can cause fission of  $^{232}\text{Th}$  besides activation to produce  $^{233}\text{U}$  at lower energy. Thus, it is important to measure the yields of the fission products in the high-energy, neutron-induced fission of  $^{232}\text{Th}$ . The yields of short-lived fission products and independent yields of various fission products are important for decay heat calculation. Further, the yields of fission products are also needed for mass and charge distribution studies, which can provide valuable information for understanding the nuclear fission process.

A literature survey<sup>6–16</sup> indicates that sufficient data in the reactor neutron-induced fission<sup>6–8</sup> and monoenergetic

neutron-induced fission<sup>9–13</sup> of  $^{232}\text{Th}$  are available in a wide range of energy from 1 to 14.8 MeV. From these data, it is found that the fission yields for 3-MeV (Ref. 9) to 14.8-MeV (Refs. 10 through 13) monoenergetic neutron-induced fission of  $^{232}\text{Th}$  are exhaustively available. Other monoenergetic neutron-induced fission yields of  $^{232}\text{Th}$  are available from the work of Trochon et al.,<sup>14</sup> Glendenin et al.,<sup>15</sup> and Lam et al.<sup>16</sup> From these data, it can be seen that the peak-to-valley ratio decreases from neutron energies of 1 to 14.8 MeV. Further, it can be seen that the fine structure around mass numbers 134–135, 139–140, and 144–145 and their complementary products decreases with an increase of neutron energy. In order to examine the latter aspect, the yields of various fission products in the neutron-induced fission of  $^{232}\text{Th}$  have been determined using a recoil catcher and off-line gamma-ray spectrometric technique with flux-averaged energies of 5.42, 7.75, and 10.09 MeV. The measured fission yield data from the present work have been compared with similar data from neutron-induced fission of  $^{232}\text{Th}$  to examine the nuclear structure effect.

## II. EXPERIMENTAL METHOD

The experiment was carried out using the 14UD BARC-TIFR [Bhabha Atomic Research Centre–Tata Institute of Fundamental Research] Pelletron facility at Mumbai, India. The neutron beam was obtained from the  $^7\text{Li}(p,n)$  reaction<sup>17</sup> by using the proton beam main line 6 m above the analyzing magnet of the Pelletron facility to utilize the maximum proton current from the accelerator. The proton energy spread at 6 m was 50 to 90 keV maximum. At this port, the terminal voltage was regulated by GVM mode using terminal potential stabilizer. Further, we used a collimator of 6-mm diameter before the target. The lithium foil was made up of natural lithium with a thickness of  $3.7\text{ mg/cm}^2$ , sandwiched between two tantalum foils of different thicknesses. The front tantalum foil facing the proton beam was the thinnest one, with a thickness of  $3.9\text{ mg/cm}^2$ , in which degradation of proton energy was only 30 keV (Ref. 18). On the other hand, the back tantalum foil was the thickest (0.025 mm), which was sufficient to stop the proton beam. Behind the Ta-Li-Ta stack, the sample used for irradiation was natural  $^{232}\text{Th}$  metal foil, which was wrapped with 0.025-mm-thick aluminum foil. The aluminum wrapper was used to stop and collect the fission products recoiling out from the surface. The size of the  $^{232}\text{Th}$  metal foil was  $1.0\text{ cm}^2$  with a thickness of  $29.3\text{ mg/cm}^2$ . The  $^{232}\text{Th}$  metal foil wrapped with aluminum was mounted at 0 deg with respect to the beam direction at a distance 2.1 cm from the location of the Ta-Li-Ta stack. A schematic diagram of the Ta-Li-Ta stack and the  $^{232}\text{Th}$  metal foil is given in Fig. 1. Different sets of samples were made for different irradiations at various neutron energies.

The Ta-Li-Ta and the  $^{232}\text{Th}$  metal foils were irradiated at proton energies ( $E_p$ ) of 7.8, 12.0, and 18.0 MeV for a period of 15, 6, and 5 h, respectively, depending upon the energy of proton beam facing the tantalum target. The proton current during the irradiations varied from 100 to 400 nA. After irradiation, the samples were cooled for 1 h. Then, the irradiated target of Th along with the Al wrapper was mounted on a Perspex plate and taken for gamma-ray spectrometry. The gamma rays of the fission/reaction products from the irradiated Th sample were counted in an energy- and efficiency-calibrated,  $80\text{-cm}^3$  high-purity germanium detector coupled to a personal computer-based 4K channel analyzer. The counting dead time was kept always  $<5\%$  by placing the irradiated Th sample at a suitable distance from the detector to avoid pileup effects. The energy and efficiency calibration of the detector system was done by counting the gamma-ray energies of the standard  $^{152}\text{Eu}$  source keeping the same geometry, where the summation error was negligible. This was checked by comparing the efficiency obtained from gamma-ray counting of standards such as  $^{241}\text{Am}$  (59.5 keV),  $^{133}\text{Ba}$  (80.9, 276.4, 302.9, 356.0, and 383.8 keV),  $^{137}\text{Cs}$  (661.7 keV),  $^{54}\text{Mn}$  (834.6 keV), and  $^{60}\text{Co}$  (1173 and 1332.5 keV). The detector efficiency was 20% at 1332.5 keV relative to the 3-in.-diam  $\times$  3-in.-long NaI(Tl) detector. The uncertainty in the efficiency was 2% to 3%. The resolution of the detector system had a full-width at half-maximum of 1.8 keV at 1332.5 keV of  $^{60}\text{Co}$ . The gamma-ray counting of the irradiated Th sample was done up to a few months to check the half-lives of the nuclides of interest.

## III. ANALYSIS OF EXPERIMENT

### III.A. Calculation of Neutron Energy

In the present experiment, the incident proton energies were 7.8, 12.0, and 18.0 MeV. The degradation

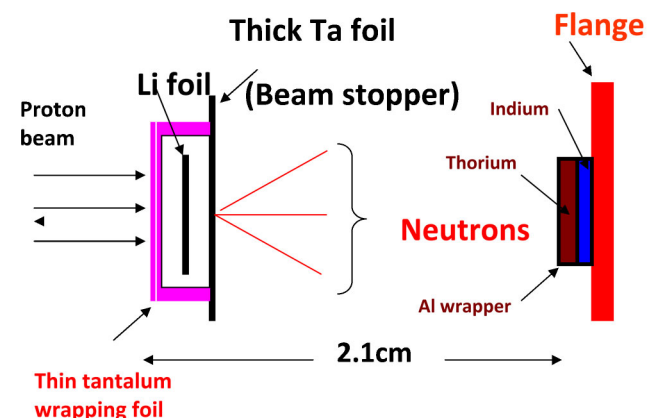


Fig. 1. Schematic diagram showing the arrangement used for neutron irradiation.

of the proton energy in the front thin tantalum foil was only 50 to 80 keV. The  $Q$ -value for the  ${}^7\text{Li}(p,n){}^7\text{Be}$  reaction to the ground state is  $-1.644$  MeV, whereas the first excited state is at  $0.431$  MeV above the ground state leading to the  $Q$ -value  $-2.079$  MeV. Therefore, for the proton energies of  $7.8$ ,  $12.0$ , and  $18.0$  MeV, the resulting peak energies for the first group of neutrons ( $n_0$ ) are  $5.92$ ,  $10.12$ , and  $16.12$  MeV, respectively. The corresponding neutron energies of the second group of neutrons ( $n_1$ ) for the first excited state of  ${}^7\text{Be}$  are  $5.42$ ,  $9.63$ , and  $15.62$  MeV for the proton energies of  $7.8$ ,  $12.0$ , and  $18.0$  MeV, respectively. Poppe et al.<sup>19</sup> have given the branching ratio to the ground state and the first excited state of  ${}^7\text{Be}$  for  $E_p = 4.2$  to  $26.0$  MeV. Further, the fragmentation of  ${}^8\text{Be}$  to  ${}^4\text{He} + {}^3\text{He} + n$  ( $Q = -3.23$  MeV) occurs, and the other reaction channel opens to give a continuous neutron energy distribution besides the  $n_0$  and  $n_1$  groups of neutrons above  $E_p = 4.5$  MeV. To observe the trend of a continuous neutron spectrum besides from  $n_0$  and  $n_1$  groups of neutrons for the proton energies of  $7.8$ ,  $12.0$ , and  $18.0$  MeV, the neutron spectrum has been generated<sup>20,21</sup> using the neutron energy distribution given by Poppe et al. Typical neutron spectra from the  ${}^7\text{Li}(p,n)$  reaction for the proton energies of  $7.8$ ,  $12.0$ , and  $18.0$  MeV are shown in Figs. 2, 3, and 4, respectively. Based on the neutron spectra, the flux-weighted average neutron energies have been calculated as  $5.42$ ,  $7.75$ , and  $10.09$  MeV for the proton energies of  $7.8$ ,  $12.0$ , and  $18.0$  MeV, respectively.

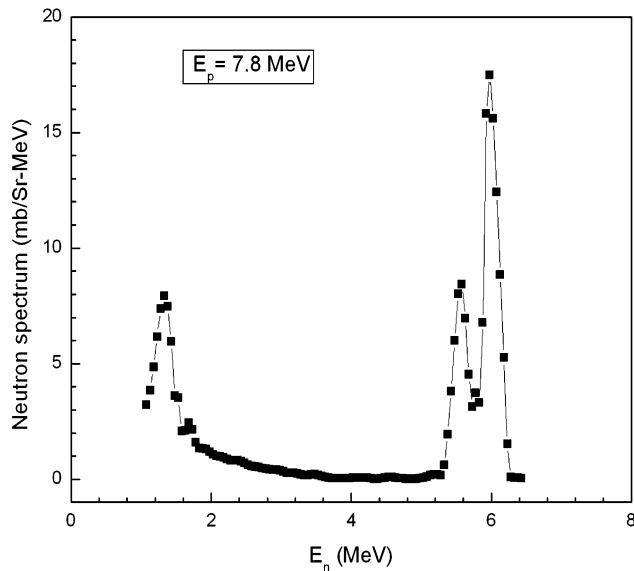


Fig. 2. Neutron spectrum from  ${}^7\text{Li}(p,n)$  reaction at  $E_p = 7.8$  MeV calculated using the results of Poppe et al.

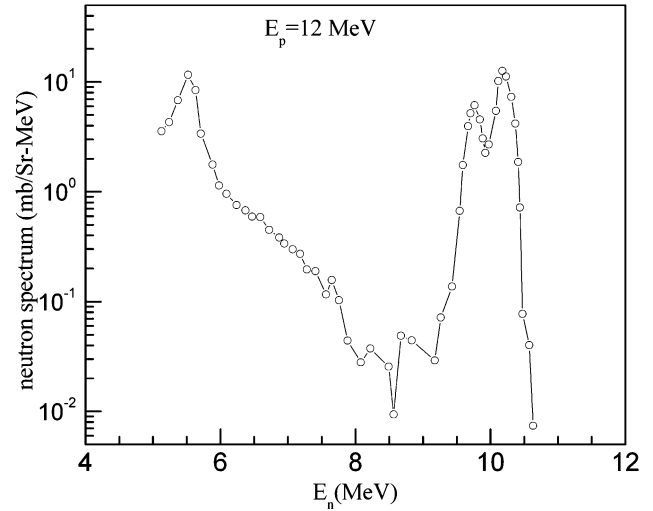


Fig. 3. Neutron spectrum from  ${}^7\text{Li}(p,n)$  reaction at  $E_p = 12.0$  MeV calculated using the results of Poppe et al.

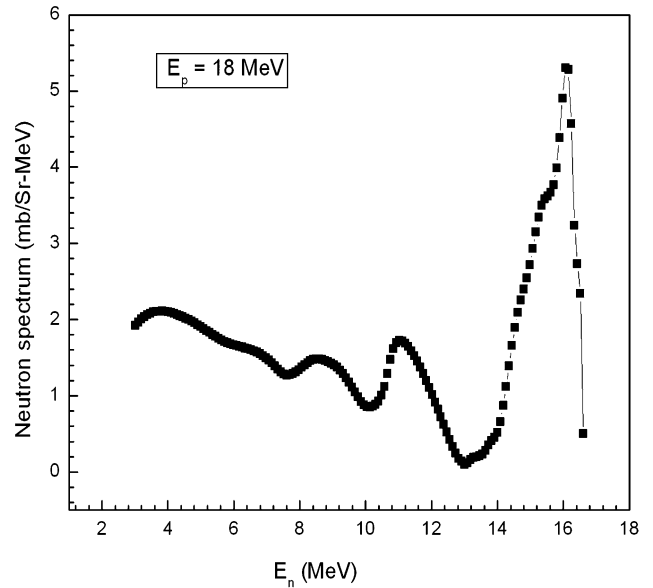


Fig. 4. Neutron spectrum from  ${}^7\text{Li}(p,n)$  reaction at  $E_p = 18.0$  MeV calculated using the results of Poppe et al.

### III.B. Calculation of Fission Yields

The photopeak areas of different gamma rays of interest were calculated by subtracting the linear background from their net peak areas. The number of gamma rays detected ( $A_{obs}$ ) under the photopeak of each individual fission product is related to the cumulative yield ( $Y_c$ ) with the following relation:

$$A_{obs}(CL/LT) = N\sigma_f(E)\phi I_\gamma \varepsilon Y_c(1 - e^{-\lambda t})e^{-\lambda T_c}(1 - e^{-\lambda LT})/\lambda, \quad (1)$$

where

$N$  = number of target atoms

$\sigma_f(E)$  = neutron-induced fission cross section as a function of neutron energy ( $E$ ) of the target with average neutron flux ( $\phi$ )

$I_\gamma$  = branching intensity for the gamma ray of the fission product

$\varepsilon$  = efficiency

$t$  = irradiation time

$T_c$  = cooling time

$CL, LT$  = clock time and live time of counting, respectively.

The nuclear spectroscopic data such as the gamma-ray energy, branching intensity, and half-life of the fission products were taken from Nuclear Structure and Decay data,<sup>22</sup> "NuDat" (Brookhaven National Laboratory). The cumulative yields of the fission product relative to fission rate monitor  $^{92}\text{Sr}$  were calculated using Eq. (1). The yield of fission rate monitor  $^{92}\text{Sr}$  was chosen from the point of view of the near constant yield with change of neutron energy.<sup>15</sup> For flux-averaged neutron energies of 5.42, 7.75, and 10.09 MeV, the fission yield data of  $^{92}\text{Sr}$  in the neutron-induced fission of  $^{232}\text{Th}$  with neutron energies of 5.9, 7.6, and 8.0 MeV were taken from Glendenin et al.<sup>15</sup>

#### IV. RESULTS AND DISCUSSION

The cumulative yields of various fission products relative to  $^{92}\text{Sr}$  in the neutron-induced fission of  $^{232}\text{Th}$  at

flux-averaged neutron energies of 5.42, 7.75, and 10.09 MeV along with nuclear spectroscopic data are given in Tables I, II, and III, respectively. The uncertainties associated with the measured cumulative yields come from the combination of two experimental data sets. The overall uncertainty is the quadratic sum of both statistical and systematic errors. The random error in the observed activity is particularly due to counting statistics and is estimated to be 5% to 10%. This can be accumulating the data for an optimum time period that depends on the half-life of the nuclide of interest. The systematic errors are due to uncertainties in neutron flux estimation (~4%), irradiation time (~1%), detector efficiency (~5%), the half-life of fission products, and gamma-ray abundances (~2%). The overall uncertainty is found to range between 8% to 12%, coming from the combination of statistical error of 5% to 10% and a systematic error of 6%.

The experimentally measured fission yield data for flux-averaged energies of 5.42 and 7.75 MeV from the present work have been compared with the available literature data<sup>15</sup> and are given in Tables I and II. The cumulative yields of different fission products in the neutron-induced fission of  $^{232}\text{Th}$  were determined for the first time at the flux-averaged energy of 10.09 MeV, and they are given in Table III. It can be seen from Tables I and II that the cumulative fission yields determined from the present work at two different flux-averaged neutron energies are in general agreement with the literature data<sup>15</sup> based on neutron-induced fission of  $^{232}\text{Th}$ . The yields of a fewer number of fission products with a decrease of neutron energy may be due to a lower neutron flux and decrease of fission cross section at the lower neutron energy of 5.42 MeV. This may also be due the tailing in the neutron energy spectrum as shown in Figs. 2, 3, and 4. In spite of the tailing of neutron energy, the yields of fission products are as many as 16 at the flux-averaged neutron energy of 10.09 MeV. The yields

TABLE I

Fission Product Yields in Neutron-Induced Fission of  $^{232}\text{Th}$  with Average Energy of 5.42 MeV

Nuclide	Half-Life	Gamma-Ray Energy (keV)	Gamma Abundance (%)	Fission Yield (%) at 5.42 MeV	
				Present Data	Glendenin et al. at 5.9 MeV (Ref. 15)
$^{91}\text{Sr}$	9.63 h	749.8	23.3	$5.37 \pm 0.59$	$6.63 \pm 0.21$
$^{92}\text{Sr}$	2.71 h	1384.9	90.0	$6.56 \pm 0.78$	$6.56 \pm 0.81$
$^{97}\text{Zr}$	16.74 h	743.3	93.03	$5.01 \pm 0.30$	$4.80 \pm 0.13$
$^{99}\text{Mo}$	65.97 h	140.5	89.4	$3.49 \pm 0.12$	$3.79 \pm 0.23$
$^{132}\text{Te}$	3.204 days	228.1	88.0	$4.01 \pm 0.48$	$3.80 \pm 0.13$
$^{133}\text{I}$	20.8 h	529.9	87.0	$3.65 \pm 0.25$	$5.64 \pm 0.19$
$^{135}\text{I}$	6.57 h	1131.5	22.6	$6.16 \pm 0.23$	$5.98 \pm 0.19$
		1260.4	28.7	$5.77 \pm 0.32$	

TABLE II  
Fission Product Yields in Neutron-Induced Fission of <sup>232</sup>Th with Average Energy of 7.75 MeV

Nuclide	Half-Life	Gamma-Ray Energy (keV)	Gamma Abundance (%)	Fission Yield (%) at 7.75 MeV	
				Present Data	Glendenin et al. at 7.6 MeV (Ref. 15)
<sup>85m</sup> Kr	4.48 h	151.1	75.0	4.59 ± 0.27	6.01 ± 0.26
<sup>87</sup> Kr	76.3 min	402.5	50.0	5.35 ± 0.32	7.10 ± 0.35
<sup>88</sup> Kr	2.84 h	196.3	26.0	5.77 ± 0.46	7.03 ± 0.30
<sup>91m</sup> Y	49.71 min	555.5	95.0	5.45 ± 0.35	
<sup>91</sup> Sr	9.63 h	749.8	23.3	6.54 ± 0.58	7.15 ± 0.21
		1024.0	33.0	6.50 ± 0.71	
<sup>92</sup> Sr	2.71 h	1384.9	90.0	6.45 ± 0.53	6.45 ± 0.78
<sup>97</sup> Zr	16.9 h	743.3	93.03	2.51 ± 0.12	3.62 ± 0.13
<sup>99</sup> Mo	65.97 h	140.5	89.4	2.38 ± 0.35	2.21 ± 0.13
<sup>132</sup> Te	3.204 days	228.1	88.0	3.09 ± 0.18	2.78 ± 0.11
<sup>133</sup> I	20.8 h	529.9	87.0	3.06 ± 0.14	4.34 ± 0.14
<sup>135</sup> I	6.57 h	1131.5	22.6	4.17 ± 0.25	5.49 ± 0.16
		1260.4	28.7	3.83 ± 0.42	
<sup>139</sup> Ba	83.03 min	165.8	23.7	6.29 ± 0.42	7.49 ± 0.63
<sup>142</sup> La	91.1 min	641.2	47.4	6.34 ± 0.24	7.01 ± 0.43
<sup>143</sup> Ce	33.03 h	293.2	42.8	7.51 ± 0.35	6.95 ± 0.41

of various fission products at the flux-averaged neutron energies of 5.42 and 7.75 MeV from the present work and comparable neutron energy from the literature<sup>15</sup> are plotted in Figs. 5 and 6. It can be seen from Figs. 5 and

6 that the higher yields of fission products around mass numbers of 134-135, 139-140, and 144-145 and their complementary products are clearly observed. In order to examine this aspect better, it is necessary to have more

TABLE III  
Fission Product Yields in Neutron-Induced Fission of <sup>232</sup>Th with Average Energy of 10.09 MeV

Nuclide	Half-Life	Gamma-Ray Energy (keV)	Gamma Abundance (%)	Fission Yield (%) at 10.09 MeV
				Present Data
<sup>77</sup> Ge	11.3 h	416.3	21.8	3.15 ± 0.16
<sup>85m</sup> Kr	4.48 h	151.1	75.0	4.72 ± 0.42
<sup>87</sup> Kr	76.3 min	402.5	50.0	5.31 ± 0.39
<sup>88</sup> Kr	2.84 h	196.3	26.0	5.56 ± 0.32
<sup>91m</sup> Y	49.71 min	555.5	95.0	7.61 ± 0.53
<sup>91</sup> Sr	9.63 h	749.8	23.3	6.60 ± 0.28
		1024.0	33.0	7.43 ± 0.56
<sup>92</sup> Sr	2.71 h	1384.9	90.0	6.62 ± 0.64
<sup>97</sup> Zr	16.9 h	743.3	93.03	3.53 ± 0.43
<sup>99</sup> Mo	65.97 h	140.5	89.0	1.81 ± 0.05
<sup>132</sup> Te	3.204 days	228.1	88.0	2.90 ± 0.23
<sup>133</sup> I	20.8 h	529.9	87.0	3.27 ± 0.31
<sup>135</sup> I	6.57 h	1131.5	22.6	4.45 ± 0.26
		1260.4	28.7	5.19 ± 0.42
<sup>139</sup> Ba	83.03 min	165.8	23.7	5.71 ± 0.32
<sup>140</sup> La	1.67 days	487.0	45.5	5.45 ± 0.61
<sup>142</sup> La	91.1 min	641.2	47.4	5.54 ± 0.29
<sup>143</sup> Ce	33.03 h	293.3	42.8	5.18 ± 0.34

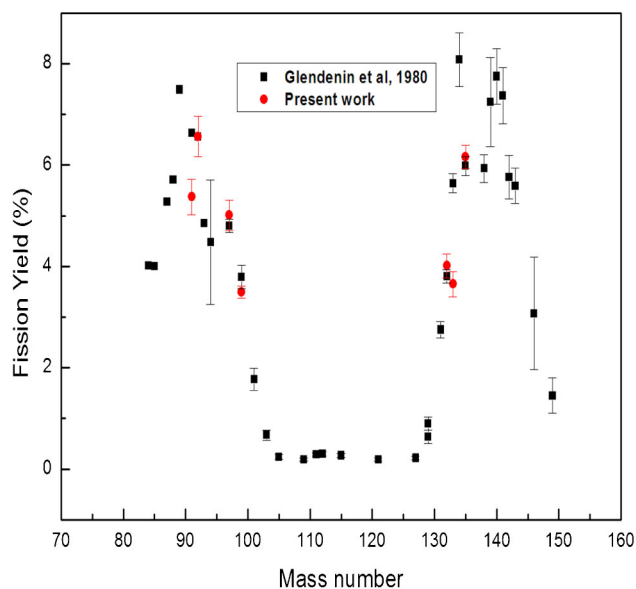


Fig. 5. Yields of fission products (%) as a function of mass number in the neutron-induced fission of  $^{232}\text{Th}$  at flux-averaged energy of 5.42 MeV along with the literature data.

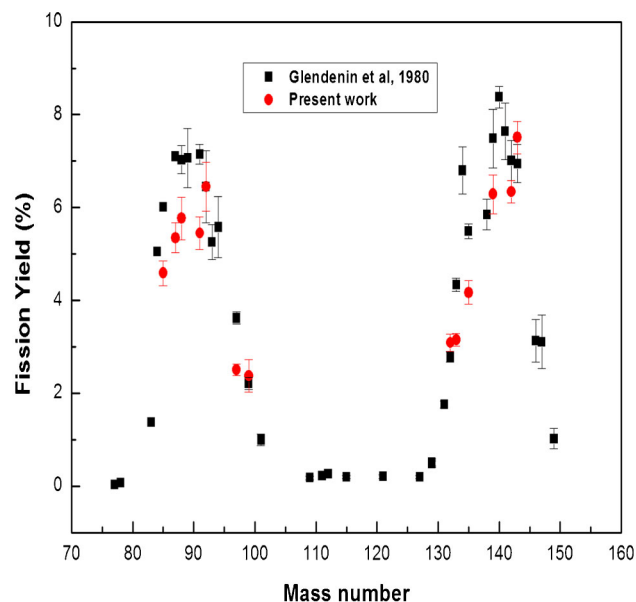


Fig. 6. Yields of fission products (%) as a function of mass number in the neutron-induced fission of  $^{232}\text{Th}$  at flux-averaged energy of 7.75 MeV along with the literature data.

data around the aforementioned mass region. The yields of 17 fission products for the flux-averaged neutron energy of 10.09 MeV are plotted in Fig. 7, and they have been determined for the first time.

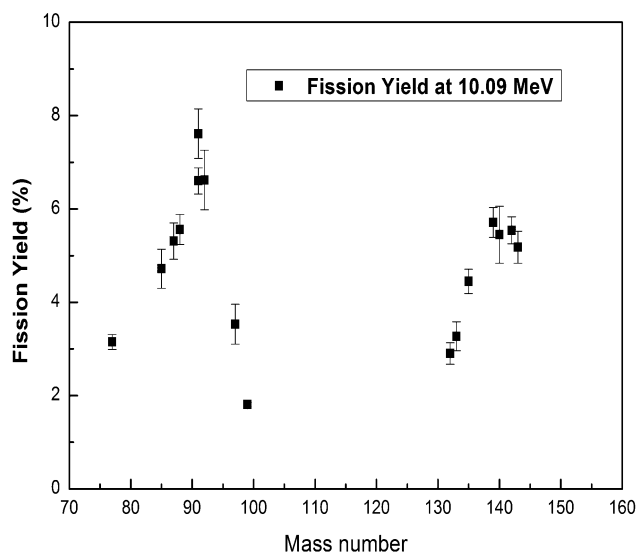


Fig. 7. Yields of fission products (%) as a function of mass number in the neutron-induced fission of  $^{232}\text{Th}$  at flux-averaged energy of 10.09 MeV.

## V. CONCLUSIONS

In the present work, the yields of 7, 14, and 16 fission products in neutron-induced fission of  $^{232}\text{Th}$  at flux-averaged neutron energies of 5.42, 7.75, and 10.09 MeV are determined using a recoil catcher and off-line gamma-ray spectrometric technique. The yields of fission products at the flux-averaged neutron energy of 10.09 MeV are determined for the first time.

The present data at flux-averaged neutron energies of 5.42, 7.75, and 10.09 MeV are in general agreement with the literature data from the neutron-induced fission data of  $^{232}\text{Th}$  at 5.9, 7.6, and 8.0 MeV, respectively.

The yields of fission products around mass numbers 134-135, 139-140, and 144-145 and their complementary products are slightly higher than the yields of other fission products. This shows the effect of nuclear structure even at higher neutron energy.

## ACKNOWLEDGMENT

The authors are thankful to the staff of the TIFR-BARC Pelletron facility for their kind cooperation and help in providing the proton beam for the experiment. We are also thankful to A. Mahadakar and D. Thapa from the target laboratory of the Pelletron facility at TIFR for providing us the Li and Ta targets. The authors P. M. Prajapati and S. Mukherjee gratefully acknowledge the Department of Atomic Energy Board of Research in Nuclear Sciences, Mumbai, for the financial support given to the M. S. University of Baroda, Vadodara, through a major research project (No. 2008/36/27-BRNS/1844).

## REFERENCES

1. S. S. KAPOOR, "Accelerator-Driven Sub-Critical Reactor System (ADS) for Nuclear Energy Generation," *Pramana J. Phys.*, **59**, 941 (2002).
2. F. CARMINATI et al, "An Energy Amplifier for Cleaner and Inexhaustible Nuclear Energy Production Driven by Particle Beam Accelerator," CERN/AT/93-47 (ET), CERN (1993).
3. C. RUBIA et al, "Conceptual Design of a Fast Neutron Operated High Power Energy Amplifier," CERN/AT/95-44 (ET), CERN (1995); see also CERN/AT/95-53 (ET), CERN (1995); see also CERN/LHC/96-01 (LET), CERN (1996); see also CERN/LHC/97- 01 (EET), CERN (1997).
4. C. D. BOWMAN, "Accelerator-Driven Systems for Nuclear Waste Transmutation," *Ann. Rev. Nucl. Part. Sci.*, **48**, 505 (1998); <http://dx.doi.org/10.1146/annurev.nucl.48.1.505>.
5. S. GANESAN, "Nuclear Data Requirements for Accelerator Driven Sub-Critical Systems—A Roadmap in the Indian Context," *Pramana J. Phys.*, **68**, 257 (2007); <http://dx.doi.org/10.1007/s12043-007-0029-1>.
6. H. N. ERTEN et al, "Mass Distribution in the Reactor-Neutron-Induced Fission of Thorium-232," *Nucl. Sci. Eng.*, **79**, 167 (1981).
7. R. H. IYER et al, "Fission of  $^{232}\text{Th}$  by Reactor Neutrons: Mass-Yield Curve," *J. Inorg. Nucl. Chem.*, **25**, 465 (1963); [http://dx.doi.org/10.1016/0022-1902\(63\)80230-4](http://dx.doi.org/10.1016/0022-1902(63)80230-4).
8. A. TURKEVICH and J. B. NIDAY, "Radiochemical Studies on the Fission of  $^{232}\text{Th}$  with Pile Neutrons," *Phys. Rev.*, **84**, 52 (1951); <http://dx.doi.org/10.1103/PhysRev.84.52>.
9. K. M. BROOM, "2.95 MeV and 14.8 MeV Neutron-Induced Fission of  $^{232}\text{Th}$ ," *Phys. Rev. B*, **133**, 874 (1964).
10. R. GANAPATHY and P. K. KURODA, "Mass Distribution in the Fission of  $^{232}\text{Th}$  by 14.8 Neutrons," *J. Inorg. Nucl. Chem.*, **28**, 2071 (1966); [http://dx.doi.org/10.1016/0022-1902\(66\)80090-8](http://dx.doi.org/10.1016/0022-1902(66)80090-8).
11. T. MO and M. N. RAO, "Symmetric Fission of  $^{232}\text{Th}$  by 14 MeV Neutrons," *J. Inorg. Nucl. Chem.*, **30**, 345 (1968); [http://dx.doi.org/10.1016/0022-1902\(68\)80458-0](http://dx.doi.org/10.1016/0022-1902(68)80458-0).
12. L. H. GEVAERT, R. E. JERVIS, and H. D. SHARMA, "Cumulative Yields in the 14 MeV Neutron Fission of  $^{232}\text{Th}$  and  $^{238}\text{U}$  in the Symmetric Region," *Can. J. Chem.*, **48**, 641 (1970); <http://dx.doi.org/10.1139/v70-104>.
13. L. SWINDLE et al, "Mass Distribution of 3 MeV Neutron Induced Fission of  $^{232}\text{Th}$ ," *J. Inorg. Nucl. Chem.*, **33**, 3643 (1971); [http://dx.doi.org/10.1016/0022-1902\(71\)80268-3](http://dx.doi.org/10.1016/0022-1902(71)80268-3).
14. J. TROCHON et al, "Fission Properties of  $^{232}\text{Th}$ ," *Nucl. Phys. A*, **318**, 63 (1979); [http://dx.doi.org/10.1016/0375-9474\(79\)90470-6](http://dx.doi.org/10.1016/0375-9474(79)90470-6).
15. L. E. GLENDENIN et al, "Mass Distributions in Monoenergetic-Neutron-Induced Fission of  $^{232}\text{Th}$ ," *Phys. Rev. C*, **22**, 152 (1980); <http://dx.doi.org/10.1103/PhysRevC.22.152>.
16. S. T. LAM et al, "Neutron-Induced Fission of  $^{232}\text{Th}$  near Threshold," *Phys. Rev. C*, **28**, 1212 (1983); <http://dx.doi.org/10.1103/PhysRevC.28.1212>.
17. S. G. MASHNIK et al, " $^7\text{Li}(p,n)$  Nuclear Data Library for Incident Proton Energies to 150 MeV," LA-UR-00-5524, Los Alamos National Laboratory; E-print: nucl-th/0011066; see also *Proc. 4th Int. Topl. Mtg. Nuclear Applications of Accelerator Technology*, Washington, D.C., November 12–15, 2000, p. 310, American Nuclear Society (2001).
18. J. F. ZIEGLER et al, "SRIM—The Stopping and Range of Ions in Matter," *Nucl. Instrum. Methods B*, **268**, 1818 (2010); <http://dx.doi.org/10.1016/j.nimb.2010.02.091>.
19. C. H. POPPE et al, "Cross Sections for the  $^7\text{Li}(p,n)^7\text{Be}$  Reaction Between 4.2 and 26 MeV," *Phys. Rev. C*, **14**, 438 (1976); <http://dx.doi.org/10.1103/PhysRevC.14.438>.
20. H. NAIK et al, "Measurement of the Neutron Capture Cross-Section of  $^{232}\text{Th}$  Using the Neutron Activation Technique," *Eur. Phys. J. A.*, **47**, 51 (2011); <http://dx.doi.org/10.1140/epja/i2011-11051-2>.
21. P. M. PRAJAPATI et al, "Measurement of Neutron Capture Cross-Sections of  $^{232}\text{Th}$  at 5.9 MeV and 15.5 MeV," *Eur. Phys. J. A.*, **48**, 35 (2012); <http://dx.doi.org/10.1140/epja/i2012-12035-4>.
22. "NuDat," Brookhaven National Laboratory; [www.nndc.bnl.gov/nudat/](http://www.nndc.bnl.gov/nudat/) (current as of Aug. 11, 2012).